NUMERICALLY EFFICIENT TECHNIQUE FOR META-MATERIAL MODELING

Ravi K. Arya, Chiara Pelletti, and Raj Mittra[*]

EMC Lab, Department of Electrical Engineering, The Pennsylvania State University, University Park, PA 16803, USA

Abstract—In this paper we present two simulation techniques for modeling periodic structures with three-dimensional elements in general. The first of these is based on the Method of Moments (MoM) and is suitable for thin-wire structures, which could be either PEC or plasmonic, e.g., nanowires at optical wavelengths. The second is a Finite Difference Time Domain (FDTD)-based approach, which is well suited for handling arbitrary, inhomogeneous, three-dimensional periodic structures. Neither of the two approaches make use of the traditional Periodic Boundary Conditions (PBCs), and are free from the difficulties encountered in the application of the PBC, as for instance slowness in convergence (MoM) and instabilities (FDTD).

1. INTRODUCTION

Frequency Selective Surfaces (FSS) comprising of periodic arrays of metallic or dielectric elements, have been extensively developed and utilized in various applications for decades to control the transmission of electromagnetic waves [1, 2]. They are also useful as Electromagnetic Band-Gap structures(EBG) and Metamaterials, that are currently finding widespread use for various applications.

The periodic structures are typically modeled as infinite doubly-periodic arrays of scatterers, and are commonly analyzed by imposing periodic boundary conditions to a unit cell to reduce the original problem to a manageable size [3]. The conventional Method of Moments (MoM) [4, 5] is often the algorithm of choice for electromagnetic scattering problems. It also provides efficient means for simulating FSSs, given the periodic elements are PEC and not

inhomogeneous and complex objects, the latter being more amenable to convenient analysis through the use of Finite Methods.

One caveat in using the Floquet-Bloch theorem to reduce the computational domain of infinite periodic structures to a single unit cell is that it leads to a slowly convergent series [6], which requires special processing, e.g., the use of Ewald transform [7]. In addition, if the FSS elements have multi-scale features and are made of metallo-dielectric materials, the MoM matrices may suffer from ill-conditioning.

The technique proposed in this paper derives the solution to the infinite doubly-periodic problem by first characterizing the current distribution over the element via the derivation of its Characteristic Basis Functions (CBFs) [8, 9]. The solution for the periodic array is then derived by progressively enlarging the size of the truncated structure and extrapolating its solution via the use of signal processing techniques [10, 11]. The CPU time and memory requirements in this approach were shown to be considerably less than those required by commercial periodic MoM codes that utilize the periodic Green's function approach.

The ability to bypass an infinite summation, either in the spatial or spectral domains, is what leads to the computational efficiency realized by using this method. In addition, the methodology we propose is very general and is already been extended to geometries and range of incident angles that are not always easily handled by the commercial codes [12].

Next, we turn to the problem of modeling of periodic structures with inhomogeneous and complex-shaped 3D elements (see Fig. 1). It is well known that MoM-based methods can become very inefficient when handling such elements, and that 3D inhomogeneous FSS problems are more amenable to convenient analysis via the use of Finite Methods. We choose to use the Finite Difference Time Domain method for
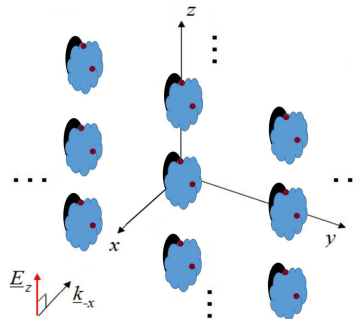

Figure 1. Representative geometry of an infinite doubly periodic array of inhomogeneous 3D elements.

this purpose, because it provides us the simulation results over a wide frequency band with a single run. We note, however, that the imposition of the PBC is not very straightforward in the FDTD, which requires a modification of the update equations when dealing with periodic structures. Furthermore, FDTD is plagued by instability issues and the update algorithm requires that the time step be progressively reduced as the angle of incidence of the plane wave impinging upon the periodic structure becomes increasingly oblique.

To obviate these difficulties, we introduce yet again a technique in this paper that bypasses the use of PBCs in the FDTD. Instead, in common with the MoM-based approach described above, we again solve the problem of a truncated periodic structure to derive the solution we seek for the original periodic structure.

Illustrative examples are also presented to demonstrate the accuracy of the approach by comparing the results derived by using a Finite Element Method (FEM) based, PBC version of the commercial code.

It is worthwhile to point out that the proposed technique is naturally suited for handling truncated periodic structures that are the starting points in the proposed approach, and are difficult to handle by using conventional methods. One of its main contributions is to show how the solution to the limiting case of infinite doubly-periodic structure can be accurately extracted from that of a corresponding finite one, whose size is relatively small.

2. PROCEDURE FOR WIRE ELEMENTS

The technique begins by applying the Characteristic Basis Function Method (CBFM) to a single unit cell of the grating (Fig. 2). The element is illuminated with a set of plane waves whose angles of incidence span the $[\theta, \phi]$ space. The number of incident angles is overestimated to capture all the possible Degrees of Freedom (DoFs)
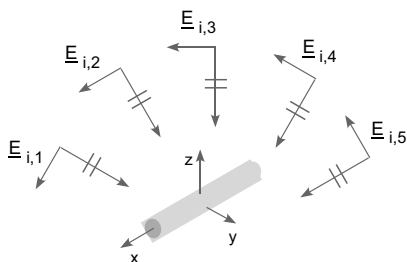

Figure 2. Geometry of the FSS unit cell with a spectrum of plane waves incident on it.

present in the solutions for the induced currents. These solutions are denoted as CBFs, namely high-level basis functions especially constructed to fit the actual geometry by incorporating the physics of the problem into their generation.

Only N linearly independent CBFs are retained for the problem at hand by applying a Singular Value Decomposition (SVD) procedure to filter out the total set of solutions. The number of surviving CBFs is relatively small, typically two or three in frequency ranges for which the size of the unit cell is smaller than one wavelength.

Once the CBFs are generated for the isolated array element, we invoke the Floquet's theorem to argue that all of the elements comprising the periodic structure must have the same current distribution, apart from a phase shift ψ which is determined by the angle of incidence of the plane wave impinging upon the grating.

Next, we construct the reduced CBF matrix $\underline{\underline{Z}}^k_{RED}$ and use it to solve a series of truncated array problems, by progressively increasing its dimension k, with the objective of predicting the asymptotic limit of the weights of the current as $k \to \infty$ and the truncated array becomes a doubly-infinite periodic structure. The reduced matrix reads:

$$
\underline{\underline{Z}}^k_{RED} = \begin{bmatrix} \left\langle \left(J^1_{CBF}\right)^t, \sum_{k=0}^R E^{s,1}_{k,CBF} \right\rangle & \cdots & \left\langle \left(J^1_{CBF}\right)^t, \sum_{k=0}^R E^{s,N}_{k,CBF} \right\rangle \\ \vdots & \ddots & \vdots \\ \left\langle \left(J^N_{CBF}\right)^t, \sum_{k=0}^R E^{s,1}_{k,CBF} \right\rangle & \cdots & \left\langle \left(J^N_{CBF}\right)^t, \sum_{k=0}^R E^{s,N}_{k,CBF} \right\rangle \end{bmatrix}
$$

$$
\underline{RHS} = \begin{bmatrix} \left\langle \left(J^1_{CBF}\right)^t, E^{i,1}_{PW} \right\rangle \\ \vdots \\ \left\langle \left(J^N_{CBF}\right)^t, E^{i,N}_{PW} \right\rangle \end{bmatrix}
\tag{1}
$$

As indicated in (2), the matrix elements are generated by following a Galerkin procedure applied only at the center $(0, 0)$ cell, with $E^{s,i}_{k,CBF}$ representing the field produced by i-th CBF J^i_{CBF} at $U_{0,0}$. The summation index k varies from 0 to R, where R is the number of concentric rings. The Right Hand Side (RHS) vector represents the tangential fields incident upon the center element of the array, tested with the same CBFs. The weights $\underline{w}^k$ of the CBFs are derived as functions of k, by imposing the continuity of the tangential E-fields at the center element surface:

$$
\underline{w}^k = \left(\underline{\underline{Z}}^k_{RED}\right)^{-1} \underline{RHS}
\tag{2}
$$

Finally, the resulting current distribution at the center cell is computed as a weighted linear combination of the CBFs.

2.1. Extraction of Periodic Array Result

The procedure for extracting the asymptotic value for the current distribution of the infinite array problem is based on processing the results of a relatively small-size truncated array, comprising of only a few rings. A typical behavior of the magnitude distribution of the weight coefficients of the current, as a function of the number of concentric rings ranging from 1 to 40, i.e., up to an 81×81 array, is shown in Fig. 3. We observe that the coefficients exhibit a relatively slow convergence behavior as we progressively increase the array size.
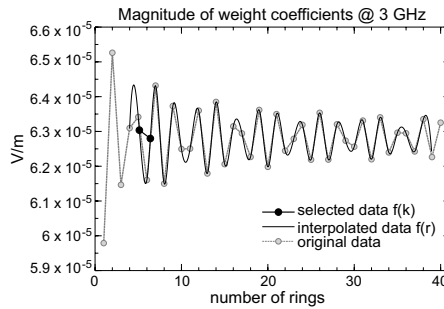
Figure 3. Magnitude variation of the current coefficients in the unit cell as functions of the size of the array, at the operating frequency of 3 GHz. Dashed marker: original data, line marker: interpolated data $f(r)$, dark round marker: $f(r)$ evaluated at first two consecutive maximum(minimum) and minimum(maximum) of its derivative ($f(k)$ at $k = k_1$ and $k = k_2$).

The method proposed herein proceeds by smoothing the magnitude and phase values of the weight coefficients through cubic spline interpolation to construct $f_m(r)$ and $f_p(r)$ for the truncated array problem. Next, we take the derivative of these functions and select a threshold t to filter out the contributions of the first $t-1$ rings which may contain artefacts. Finally, starting from $r \geq t$, we find the first two consecutive maximum (minimum) and minimum (maximum) values of $f'(r)$, which correspond to the points of which the slope of $f(r)$ is maximum. We find two consecutive indices $k = k_1$ and $k = k_2$, for which the slope is maximum, and then take the average of f values evaluated at these two points as the asymptotic value we are seeking.

The reflection and transmission coefficients are defined as:

$$\Gamma = \frac{\underline{E}^{scat}}{\underline{E}^{inc}} \quad \text{and} \quad \tau = \frac{\underline{E}^{trans}}{\underline{E}^{inc}} \tag{3}$$

where $\underline{E}^{scat}$ and $\underline{E}^{trans}$ represent the scattered and transmitted fields

in the far-region. Our final step is to work with the induced currents to derive the Γ and τ using (3), in a manner similar to that in [13].

The methods described above, for analyzing periodic structures can also be applied to problems involving plasmonic materials, such as arrays of nanorods at optical frequencies, which find a wide range of applications in photonics [14].

3. PROCEDURE FOR THREE-DIMENSIONAL STRUCTURES

We will now turn to arbitrary three-dimensional elements that are not amenable to efficient analysis by using the Method of Moments and are best handled by Finite methods, e.g., the FEM or the FDTD. The FEM analysis applied in conjunction with the Periodic Boundary Condition (PBC) is well established and will not be discussed here. The FDTD has also been applied in the past with the PBC, but is fraught with a number of difficulties, primarily encountered when the angle of incidence of the incident plane wave is not close to normal. Specifically, it is very common to run into instabilities in the FDTD time-updating process, despite the reduction of the time-step, which must be done as the incident angle becomes more and more oblique.

The method described herein not only circumvents these difficulties with the instabilities and time-step reduction, but it also does not require the introduction of auxiliary functions [15] in the FDTD update equations. As a first step, we modify the given doubly-infinite periodic structure to the truncated model as shown in Fig. 4. We place the truncated structure inside a parallel-plate waveguide; so that it remains periodic in the y-direction by virtue of imaging by the parallel planes. An incident field which is polarized in the y-direction, with its k-vector in the x-z plane, impinges upon the structure at an arbitrary angle relative to the z-axis. Of course, this configuration restricts us to change the incident angle only in the x-z plane.

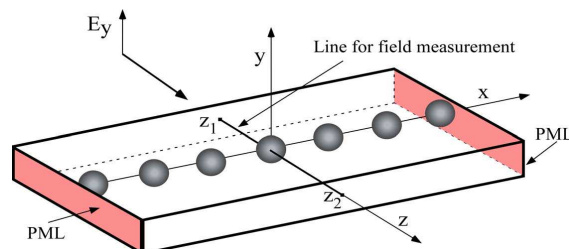The computational domain is terminated in the x-direction

Figure 4. Modified waveguide geometry.

by using Perfectly Matched Layers (PML), as is the case for the conventional FDTD.

In common with the procedure described in Section 2.1 we again truncate the doubly-periodic structure to a finite one and develop a technique for extrapolating the results of the finite structure to that of the infinite doubly-periodic geometry. However, the original approach, which was based on the extrapolation of the weight coefficient of the current distribution in the context of the Method of Moments must be tailored for the FDTD, since it deals with E and H fields, and not directly with induced currents. The details of the proposed procedure appear in Section 3.1.

3.1. FDTD-based Method for Computing Reflection and Transmission Coefficients

Our next step is to solve the waveguide structure scattering problem shown in Fig. 4 by using a Finite Method, e.g., the FDTD and to compute the scattered fields along the longitudinal direction on a line at the center of the waveguide as shown in Fig. 4.

We note that the total field on the incident side of the waveguide ($z < 0$) is a summation of the incident and scattered (reflected) fields, while only the transmitted fields exist in the forward direction ($z > 0$), as shown in Fig. 4.

Next, for the normal incidence case, we decompose the fields measured along the line z_1-z_2 (see Fig. 4) within region $z < 0$ into their incident and reflected components by using the Generalized Pencil-Of-Function (GPOF) method [16]. For the oblique incidence case, the fields are measured along specular directions both in the reflection and the transmission regions.

The weights of the transmitted and reflected fields associated with the dominant Floquet harmonic determined by the GPOF algorithm, yield the transmission and reflection coefficients for the truncated array. The reflection and transmission coefficients, computed by using (3), are tracked progressively by increasing the number of elements in the transverse direction (see Fig. 5).

Our next step is to plot Γ and τ as functions of the number of cells as shown in Fig. 5. These intermediate values are processed next to derive the asymptotic value for the reflection coefficient of the particular frequency for which we have measured the fields. This process is repeated for all the frequencies of interest and the extrapolated reflection coefficient values are plotted over the desired frequency band as shown below.
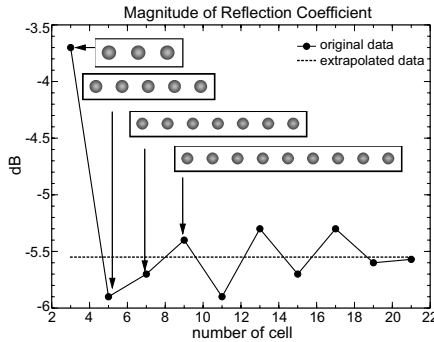
Figure 5. Magnitude of the reflection coefficient as a function of the number of elements, in the x-direction; solid line: original data, dashed: extrapolated data.

4. NUMERICAL RESULTS

For the first test example, we consider a single-layer, planar, doubly-periodic FSS of infinite extent (in the x- and y-directions) with periodicities $D_x = D_y = 0.7\lambda_0$, where λ_0 is the wavelength at 5 GHz. Each cell contains a PEC wire of $\lambda_0/2$ in length, whose radius is $\lambda_0/500$, and which is tilted *out of plane* at an angle of $\theta = 60°$ (see Fig. 6).
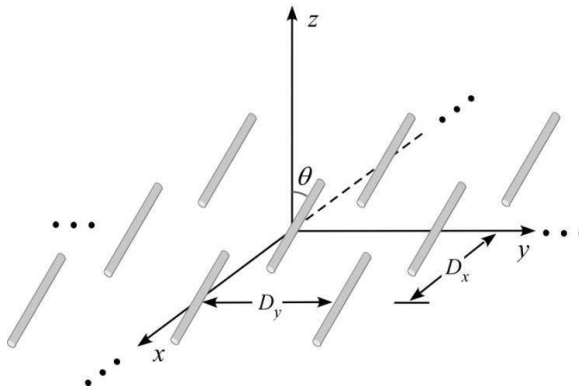

Figure 6. Representative geometry of the analyzed periodic array of dipoles tilted out-of-plane $(\theta = 60°)$.

An x-polarized plane wave, traveling along the $-z$ direction, is normally incident upon the grating. Only one CBF is found to be sufficient to describe the current distribution over this type of element; hence, the related reduced matrix is just 1×1. The frequency range of our interest spans from 3.5 to 6 GHz. The reflection and transmission
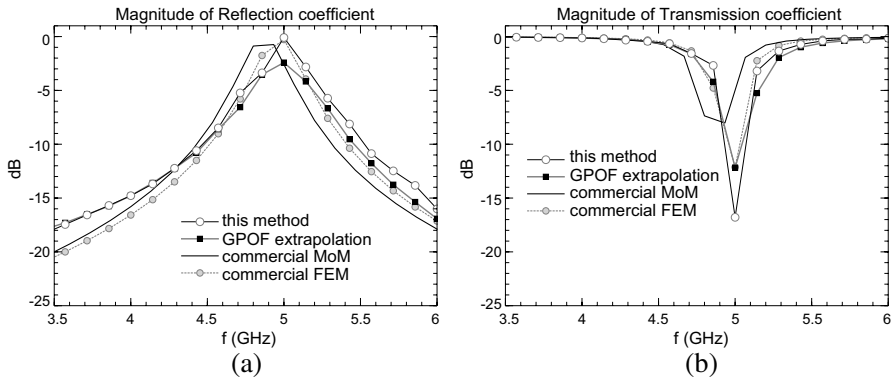
Figure 7. Magnitude of the (a) reflection coefficient and (b) transmission coefficient derived by using this method and compared with those obtained by using: GPOF extrapolation; and commercial MoM and FEM.

Table 1. Run-time performance for the dipole test example by using the present method (CBFM with truncation procedure), CBFM with GPOF extrapolation and commercial solvers implementing the MoM and the FEM.

Numerical method	This method	GPOF extrapolation	MoM	FEM
Normalized time	1	3.5	454.5	901.9

characteristics of the array are compared in Fig. 7.

The agreement with the results obtained independently by using GPOF extrapolation and software modules is seen to be good.

Table 1 below lists the time comparison, to illustrate the advantage of our method in terms of run-time, both over existing EM solvers and previous published data. The normalized time has been defined as follows:

$$\text{Norm. time} = \frac{\text{Time for other method}}{\text{Time for this method}} \qquad (4)$$

Next, we present some representative results for the reflection characteristics of 3D structures. In Fig. 8 we show the results for an array of PEC spheres whose diameters are $0.5\lambda_0$ with periodicity of $0.75\lambda_0$, at the operating frequency of 5 GHz. The array is illuminated by a plane wave at normal and 20 degree incidence angles, respectively. We also compare the obtained results against those derived by using a commercial FEM solver.

As it is well known, the FDTD can handle dielectric and PEC

structures with ease, Fig. 9 shows the results for an array of dielectric spheres with $\epsilon_r = 9$ and diameters of $0.5\lambda_0$ with periodicity of $0.75\lambda_0$ at the operating frequency of $5\,\mathrm{GHz}$. Again, the results have been derived for normal and 20 degree incidence angles, respectively.

Figure 10 also shows the results for PEC spheres coated with a dielectric layer, whose ϵ_r is 9. For this case, the PEC spheres have diameters of $0.5\lambda_0$ and a periodicity of $0.75\lambda_0$ at the operating frequency of $5\,\mathrm{GHz}$. The thickness of the dielectric is $\lambda_0/20$.
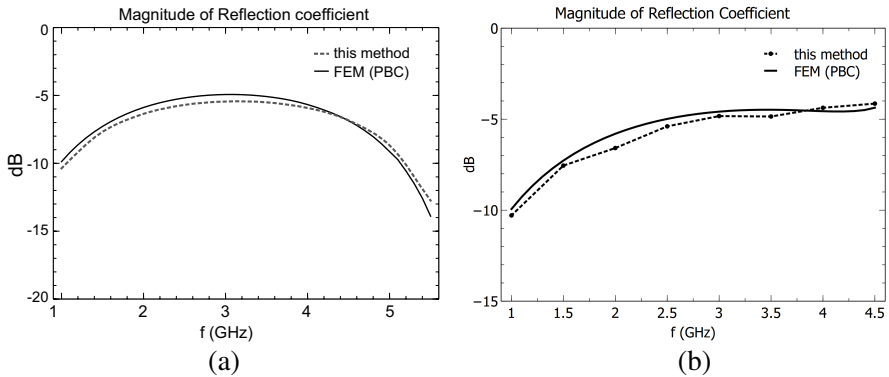

Figure 8. Magnitude of Reflection coefficient for (a) normal incidence and (b) 20 degrees incidence, derived by using the present method and compared with those from a commercial FEM (PBC) solver for PEC spheres.
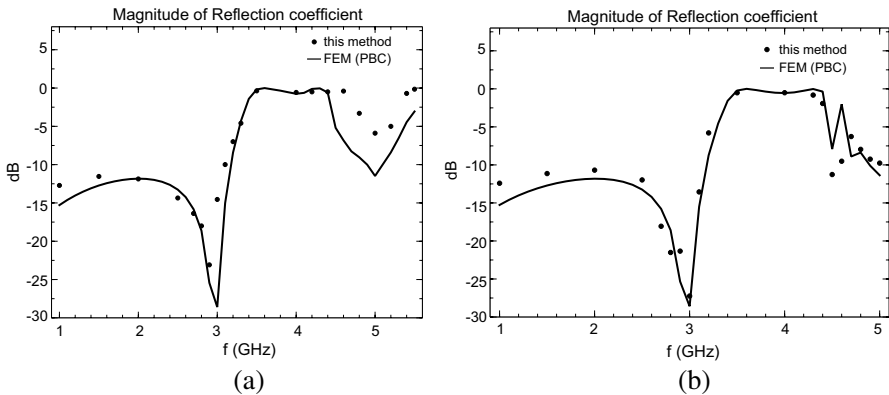

Figure 9. Magnitude of Reflection coefficient for (a) normal incidence and (b) 20 degrees incidence, derived by using the present method and compared with those from a commercial FEM (PBC) solver for dielectric spheres.
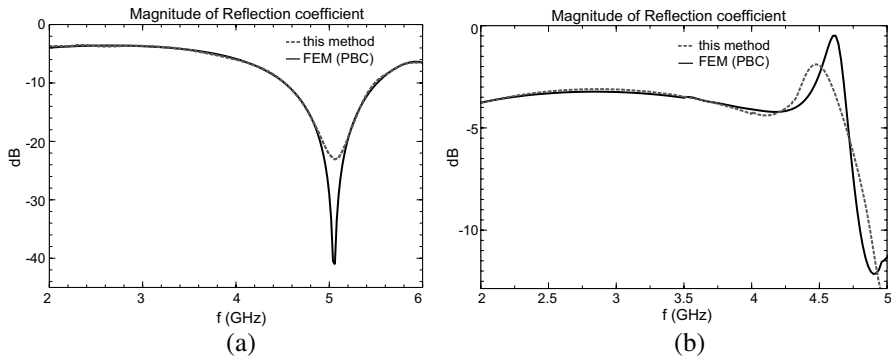
Figure 10. Magnitude of Reflection coefficient for (a) normal incidence and (b) 20 degrees incidence, derived by using the present method and compared with those from a commercial FEM (PBC) solver for PEC spheres coated with dielectric material.

To further illustrate the versatility of this method, we have applied this technique to FSSs with 3D elements [17], as shown in Fig. 11. This structure is somewhat different from the one presented in [17], in that it is tuned to a different frequency and is implemented with flat strips — as opposed to wires-supported by RO4003 ($\epsilon_r = 3.55$) dielectric layer of thickness d. The flat strips at the top and bottom are connected by vias, as shown in Fig. 11(a). Fig. 12 shows the transmission coefficient of this structure. We note that there is slight difference at the low end of the frequency band between the simulated and measured results, and that the measured result shows a slightly wider bandwidth than the simulated one. This difference could be due to tolerances in the fabricated model, as well as due to conductor losses in the structure. It is interesting to note, however, that our results are closer to the measured ones than those predicted by the commercial FEM (PBC) code.

It is evident from Figs. 8, 9, 10 and 12 that good agreement has been achieved between the results obtained from a commercial FEM solver and the proposed algorithm, despite the fact the use of PBCs is totally avoided in the present method and, hence, concerns regarding instability and reduction in the time step are obviated. As mentioned earlier, working in the time domain, as we have done in the proposed method, enables us to generate the solution over a frequency band with a single run, but without the burden of instability and numerical inefficiency that plague the conventional FDTD/PBC analysis.
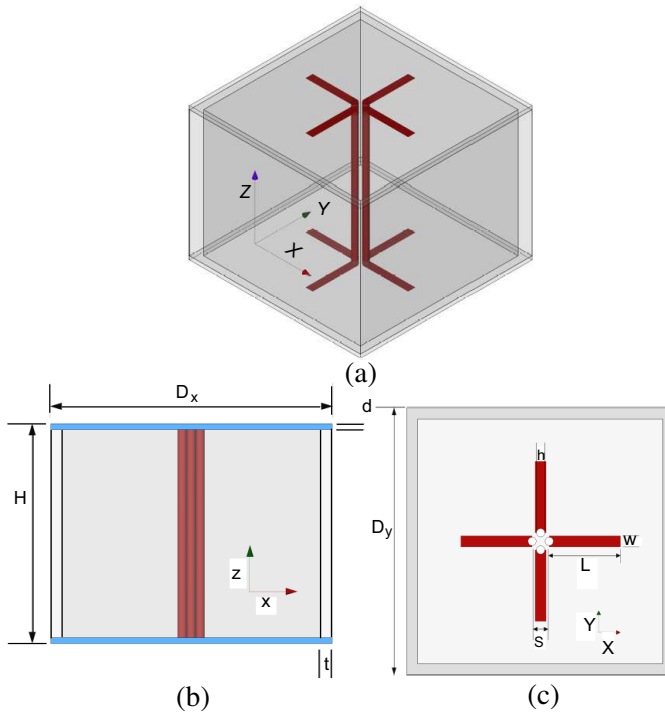
(a)

(b)

(c)

Figure 11. Geometry of analyzed FSS unit cell. (a) 3D view, (b) side view, (c) top view. Geometry parameters are: $H = 18.96$ mm, $d = 0.508$ mm, $t = 1$ mm, $w = 1$ mm, $s = 2 * 0.784$ mm, $h = 0.76$ mm, $L = 6.5$ mm and periodicity $D_x = D_y = 24.29$ mm.
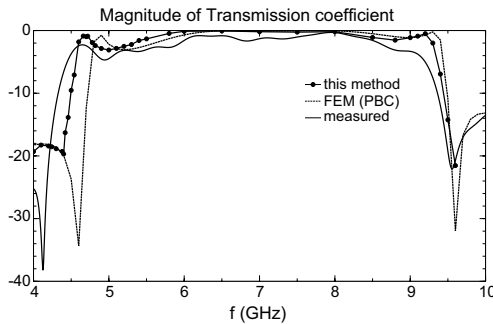

Figure 12. Magnitude of transmission coefficient for normal incidence from the present method, a commercial FEM (PBC) solver and measured results.

5. CONCLUSIONS

In this paper, we have introduced two simulation techniques for modeling periodic structures with three-dimensional elements. The proposed first technique yields accurate results for the reflection and transmission characteristics of the array, at a fraction of the computational cost when compared to those required by existing codes for modeling periodic structures. The computational efficiency is realized by totally bypassing the evaluation of the infinite summations, either in the spatial or in the spectral domains. Also, we have introduced a second technique to derive the response characteristics of periodic arrays characterized by arbitrary 3D type of elements. This method yields results that are in good agreement with those obtained from commercial solvers, while it avoids the use of PBCs, thus bypassing the difficulties encountered in the FDTD with the increase in the solve-time, and with issues pertaining to the stability behavior.

Before closing, we mention that the techniques presented herein can be modified to address the important problem of modeling periodic structures with statistical variations in their geometries, as is typically the case with MTMs for optical wavelengths, where the difficulties in their fabrication almost always introduce small variations in the dimensions of the elements that comprise the periodic array.

REFERENCES

1. Mittra, R., C. H. Chan, and T. Cwik, "Techniques for analyzing frequency selective surfaces — A review," *IEEE Proc.*, Vol. 76, No. 12, 1593–1615, 1998.
2. Wu, T. K., *Frequency Selective Surface and Grid Array*, John Wiley & Sons Inc., 1995.
3. Munk, B. A., *Frequency Selective Surfaces: Theory and Design*, Wiley, New York, 2000.
4. Peterson, A. F., S. L. Ray, and R. Mittra, *Computational Methods for Electromagnetics*, IEEE Press, New York, 1998.
5. Harrington, R. F., *Field Computation by Moment Method*, The Macmillan Company, New York, 1968.
6. Blackburn, J. and L. R. Arnaut, "Numerical convergence in periodic method of moments of frequency-selective surfaces based on wire elements," *IEEE Trans. on Antennas and Propag.*, Vol. 53, 3308–3315, Oct. 2005.
7. Stevanovic, I., P. Crespo-Valero, K. Blagovic, F. Bongard, and J. R. Mosig, "Integral-equation analysis of 3-D metallic objects

arranged in 2-D lattices using the Ewald transformation," *IEEE Trans. on Microwave Theory and Tech.*, Vol. 54, No. 10, 3688–3697, Oct. 2006.

8. Prakash, V. V. S. and R. Mittra, "Characteristic basis function method: A new technique for efficient solution of method of moments matrix equations," *Microwave and Optical Technology Letters*, Vol. 36, No. 2, 95–100, Jan. 2003.

9. Wan, J. X., J. Lei, and C. H. Liang, "An efficient analysis of large-scale periodic microstrip antenna arrays using the characteristic basis function method," *Progress In Electromagnetics Research*, Vol. 50, 61–81, 2005.

10. Yoo, K., N. Mehta, and R. Mittra, "A new numerical technique for analysis of periodic structures," *Microwave and Optical Technology Letters*, Vol. 53, No. 10, 2332–2340, Oct. 2011.

11. Mittra, R., C. Pelletti, N. L. Tsitsas, and G. Bianconi, "A new technique for efficient and accurate analysis of FSSs, EBGs and metamaterials," *Microwave and Optical Technology Letters*, Vol. 54, No. 4, 1108–1116, Oct. 2011.

12. Mittra, R., R. K. Arya, and C. Pelletti, "A new technique for efficient and accurate analysis of arbitrary 3D FSSs, EBGs and metamaterials," *2012 IEEE Antennas and Propagation Society International Symposium (APSURSI)*, 1–2, Chicago, IL, Jul. 2012.

13. Mittra, R., C. Pelletti, N. L. Tsitsas, and G. Bianconi, "A new technique for efficient and accurate analysis of FSSs, EBGs and metamaterials," *Microwave and Optical Technology Letters*, Vol. 54, No. 4, 1108–1116, Apr. 2012.

14. Rashidi, A., H. Mosallaei, and R. Mittra, "Numerically efficient analysis of array of plasmonic nanorods illuminated by an obliquely incident plane wave using the characteristic basis function method," *J. Comput. Theor. Nanosci.*, No. 10, 427–445, 2013.

15. Taflove, A. and S. C. Hagness, *Computational Electrodynamics: The Finite-difference Time-domain Method*, 3rd Edtion, Artech House, Norwood, MA, 2005.

16. Hua, Y. and T. Sarkar, "Generalized pencil-of-functions method for extracting poles of an EM system from its transient response," *IEEE Trans. on Antennas and Propag.*, Vol. 37, No. 2, 229–234, Feb. 1989.

17. Pelletti, C. and R. Mittra, "Three-dimensional FSS elements with wide frequency and angular responses," *IEEE Antennas and Propagation Society International Symposium*, 1–2, Chicago, IL, Jul. 2012.